

Freezing of a water-saturated inclined packed bed of beads

C.-H. YANG, S. K. RASTOGI and D. POULIKAKOS

Mechanical Engineering Department, University of Illinois at Chicago, P.O. Box 4348,
Chicago, IL 60680, U.S.A.

(Received 10 April 1992 and in final form 22 September 1992)

Abstract—An experimental investigation is reported for the problem of transient freezing of an inclined water-saturated bed of beads. The effect of the inclination angle on the temperature field, the shape of the ice-water interface, the initiation time of ice nucleation, and the volume of the frozen region are obtained for two types of beds of beads with significantly different thermal conductivities (glass and steel). The dependence of the volume of the frozen region on the inclination angle and on time is summarized in engineering correlations for both the bed of glass beads and the bed of steel beads.

1. INTRODUCTION

THE FREEZING of liquid-saturated porous materials occurs in many engineering and geophysical systems. Examples of such systems include thermal energy storage [1], artificial freezing of ground used as a structural support and as a water barrier in construction and mining applications [2], natural freezing of soil [3] and food processing. Further, better knowledge of the phenomena of the freezing and thawing of liquid-saturated porous media will improve the design of ground-based heat pump systems which often use heat exchanger pipes buried underground [4, 5]. A significant complexity in the study of freezing in liquid saturated porous materials arises if convective flow is present in the liquid phase. The shape of the solid-liquid interface and the rate of freezing strongly depends on the nature of this flow.

Owing to the abundance of water in nature one often encounters freezing of a porous matrix that is saturated with water. The existing studies on freezing of water-saturated porous media can be categorized into two groups depending upon the presence or absence of seepage (forced convection flow) or natural convection flow. The results of representative works from both groups are discussed in the following paragraphs.

Goldstein and Reid [6] studied the problem of freezing of a water-saturated porous medium in the presence of seepage flow analytically. Using the methods of the complex variable theory, the energy equation in the unfrozen region was solved without prescribing the shape of the frozen region. The non-linear interfacial energy balance was transformed into a non-linear integral equation which was linearized and solved. For a similar situation, i.e. in the presence of ground water flow normal to the centerline of a pipe, Hashemi and Sliepcevich [7] conducted a numerical study using the finite element method to model the

freezing around a row of pipes. A single energy equation for the solid as well as for the liquid region was used. The latent heat effect was included through the use of a temperature-dependent specific heat. A similar study was performed by Frivik and Comini [8] to model the freezing and thawing of soil in the presence of seepage flow using a finite element method. The predicted temperature distributions were compared successfully with experimental data obtained from a laboratory model of a soil freezing system. Darcy's law was used in order to model the flow in the above studies [6–8] and natural convection was neglected. Studies on the freezing of porous media in the presence of natural convection are discussed next.

O'Neill and Albert [9] investigated the solidification of liquid-saturated porous media numerically using a finite element method. No results specific to water-saturated porous media were reported. Weaver and Viskanta [10, 11] conducted experimental and analytical studies of the freezing of a water-saturated porous medium. Experiments were performed in a cylindrical capsule cooled from the outside for vertical as well as horizontal orientations. In addition, a simple model based on conduction alone in both the liquid and the solid regions was proposed. The agreement between the analytical model and the experimental data was reported to be good for the water-glass bead system. However, for the water-aluminum bead system, the model showed significant deviation from the experimental data.

Chellaiah and Viskanta [12] studied the freezing of saturated and superheated water in porous media enclosed in a rectangular cavity. They examined the effects of the glass bead size, the imposed temperature difference and the liquid superheat. For freezing of saturated water, good agreement was reported between the experimental temperature distribution and the temperature distribution predicted by a one-dimensional heat conduction model. In a subsequent

NOMENCLATURE

| | |
|-------|--|
| C | specific heat [$\text{J kg}^{-1} \text{K}^{-1}$] |
| Fo | Fourier number, equation (1) |
| H | height of the cavity [m] |
| L | latent heat of fusion [J kg^{-1}] |
| Ste | Stefan number, equation (1) |
| t | time [s] |
| t_n | nucleation time [s] |
| T | temperature [$^{\circ}\text{C}$] |
| V | frozen solid volume [m^3] |
| V_T | total volume of the cavity [m^3] |
| V^* | dimensionless volume, V/V_T . |

Greek symbols

| | |
|----------|--|
| α | thermal diffusivity [$\text{m}^2 \text{s}^{-1}$] |
| θ | inclination angle [deg] |
| τ | dimensionless time, equation (1). |

Subscripts

| | |
|----|-----------------------------------|
| f | fusion |
| i | initial |
| m | volume-average |
| ms | volume-average in the solid phase |
| s | solid phase. |

study, Chellaiah and Viskanta [13] developed a numerical model that accounted for both conduction in the solid and natural convection in the unfrozen region. Their model was based on the volumetric averaging of the macroscopic transport equations, with phase-change assumed to occur volumetrically over a very small temperature range. In the liquid region, both the Brinkman and the Forchheimer extensions to the Darcy momentum equation were accounted for. The effect of the density inversion of water on the heat transfer and fluid flow was also modeled. The results of the numerical model were compared successfully to experimental data.

The present paper reports the results of an experimental study on the transient freezing of a bed of beads saturated with water initially at room temperature and contained in an inclined rectangular enclosure with one cooled wall and the remaining walls insulated. The entire range of inclination angles with respect to the gravity vector (0 – 180°) is examined. Key results on the temperature field, the shape of the ice–water interface, and the ice volume production are presented for two beds of beads with considerably different thermal conductivities (glass and steel, respectively). Two engineering correlations for the dependence of the frozen region volume on the inclination angle and on time are reported.

2. EXPERIMENTAL APPARATUS AND PROCEDURE

The setup for the experiment consisted of a test section and two supporting devices. The two supporting devices were a data acquisition system and a bath refrigerator circulator. The data acquisition system consisted of a Hewlett–Packard 150 Touchscreen II PC, two Hewlett–Packard 3421A data acquisition/control units, a printer, and a Hewlett–Packard data acquisition software package. A Neslab RTE-110 refrigerator unit was used to cool the cold wall of the apparatus.

Freezing experiments were conducted in a rectangular cavity (Fig. 1) with internal dimensions of

the water-saturated porous space of 51 mm in length, 51 mm in height, and 57 mm in depth. Two circular tracks were used to rotate the cavity at any desired angle. The cold wall of the test cell was manufactured out of stainless steel of thickness 6.85 mm. This wall was machined to have a counterflow heat exchanger. The counterflow heat exchanger was constructed by milling four channels into the stainless steel plate. A 50% ethylene glycol–water solution precooled by the bath circulator refrigerator was circulated through the heat exchanger. The direction of the flow of the coolant in the heat exchanger was alternated between adjacent channels to establish the isothermality of the wall. To check the uniformity of the temperature of the cooling plate, five thermocouples were installed. Indeed, the cooling plate was found to be isothermal within 0.2°C for all the experiments.

The remaining walls of the apparatus were made out of Plexiglas of a thickness of 6.85 mm. Two Plexiglas plates separated with a vacuum gap in between were used on the front and the back of the rectangular cavity so as to reduce the heat losses, to eliminate

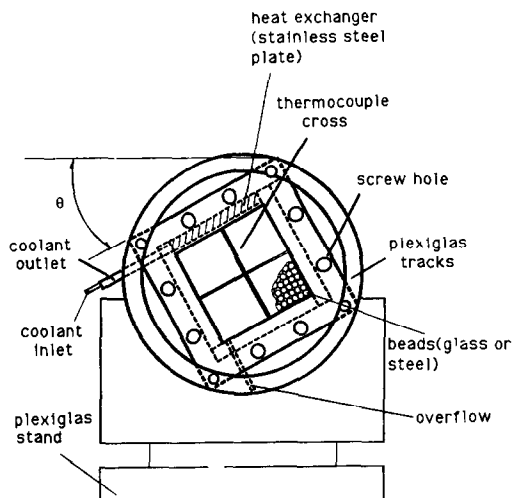


FIG. 1. Schematic of the test section.

the condensation of moisture, and to allow for the photographic observations. An additional 20 mm thick styrofoam insulation was used to surround the apparatus which helped to practically eliminate the heat losses.

A thermocouple grid consisting of a total of 20 30-gauge copper and constantan thermocouples was placed at the mid-plane of the cavity perpendicular to the cold wall (Fig. 1). The grid was cut out of a thin Plexiglas sheet in the form of a cross. The thermocouples were mounted through small holes drilled in the Plexiglas cross. There were 10 equidistant thermocouples in each direction (perpendicular and parallel to the cold wall, Fig. 1). The thermocouple wires exited the cavity through two small holes in the side walls that were sealed afterward.

Spherical soda-lime glass beads and stainless steel beads of an average diameter of 5 mm constituted the porous matrix in the two sets of experiments. Hence, the porosity and the permeability were the same in the two systems. Distilled water was used as the saturating fluid of the porous medium in all the experiments.

The procedure for obtaining the experimental data was as follows. First, the enclosure was packed completely with either the glass beads or the stainless steel beads with the thermocouple grid kept in the mid-plane perpendicular to the cold surface. Care was taken to assure the homogeneity of the porous matrix. Next, the enclosure was carefully filled with distilled water without introducing air bubbles. The apparatus was then positioned at the desired angle with respect to the gravity vector. The coolant in the refrigerator, which was precooled and kept at -25°C in all experiments, was suddenly circulated through the heat exchanger machined into the stainless steel wall of the apparatus. As a result, buoyancy-induced convection and eventually solidification took place in the water-saturated porous medium. The solidification front was observed and photographed at several time intervals. Temperature measurements were recorded at time intervals of 30 s early in the experiment and 60 s later, well after the ice formation.

The accuracy of the temperature measurements was estimated to be within 3% and was dictated by the accuracy of the software that converted the voltage measurements to temperature. The frozen solid volume was estimated by tracing the solid-liquid interface at different times and, next, by measuring the area of the frozen layer by a digital planimeter. For each solid-liquid interface location, the area of the frozen layer was measured three times. The reported data points are based on the arithmetic mean of the three readings. The photographs used to trace the solid-liquid interface were taken using a Nikon FE 35 mm camera with T-max ASA 400 black and white film.

Qualitative visualization of the flow field was performed by adding potassium permanganate crystals to the fluid. A high intensity light was placed on the opposite side of the apparatus from the observer. As

the crystals dissolved they created dark streaks that visualized the flow. The results of this simple flow visualization method allowed us to obtain a rough idea of the flow field by observation and were not meant to provide a detailed description of the fluid motion in the cavity.

3. RESULTS AND DISCUSSION

The discussion of the results starts with the dependence of the cold wall temperature on time for various inclination angles and for both the systems of interest, namely the water-glass bead system and the water-steel bead system. The temperature data are plotted vs time for all inclination angles in Fig. 2. Figure 2(a) contains the data for the glass bead bed. The data for the steel bed are shown in Fig. 2(b). Note that the temperature plotted in Fig. 2 is the arithmetic mean of the temperature recorded by the five thermocouples attached on the cold wall. Even though the temperature data were recorded for the entire duration of the experiments (90 min), Fig. 2 shows data only for the first 6 min since these data contain all the important information of the wall temperature variation. In both the above mentioned systems (Figs. 2(a) and (b)), the cold wall temperature decreases monotonically for all inclination angles until the time of the ice nucleation (formation) which is marked by a jump on the temperature curves. The rate of decrease is steeper for the glass bead bed compared to the steel bead bed. This result can be attributed to the fact that the thermal conductivity of a glass bead is nearly 30-times lower than that of a steel bead.

As mentioned earlier, the ice nucleation time is characterized by a jump on the temperature curves for all inclination angles. This jump is caused by the release of the latent heat of fusion at the cold wall when the ice first forms as well as by the fact that the solidification front is at 0°C which is higher than the cold wall temperature at the time of ice nucleation. Following the ice nucleation, the cold wall temperature decreases monotonically until it reaches practically a plateau after 6 or 7 min from the initiation of the cooling.

The dependence of the ice nucleation time on the inclination angle is reported in Fig. 3 for the glass bead bed and the steel bead bed. The ice nucleation time does not vary in a monotonic fashion with the inclination angle, θ . Interestingly, it features a minimum at $\theta \approx 60^{\circ}$ for the glass bead bed and $\theta \approx 90^{\circ}$ for the steel bed. Further, for the same inclination angle, the ice nucleation in the glass bead bed occurs faster than in the steel bed. The physical explanation for this finding is as follows. Since the thermal conductivity of steel is nearly 30-times larger than that of glass, the cooling effect of the wall propagates faster in the steel beads than in the glass beads. In the later case it is felt for a longer time in the vicinity of the cold wall aiding the initiation of ice formation. The dependence of the nucleation time on the inclination

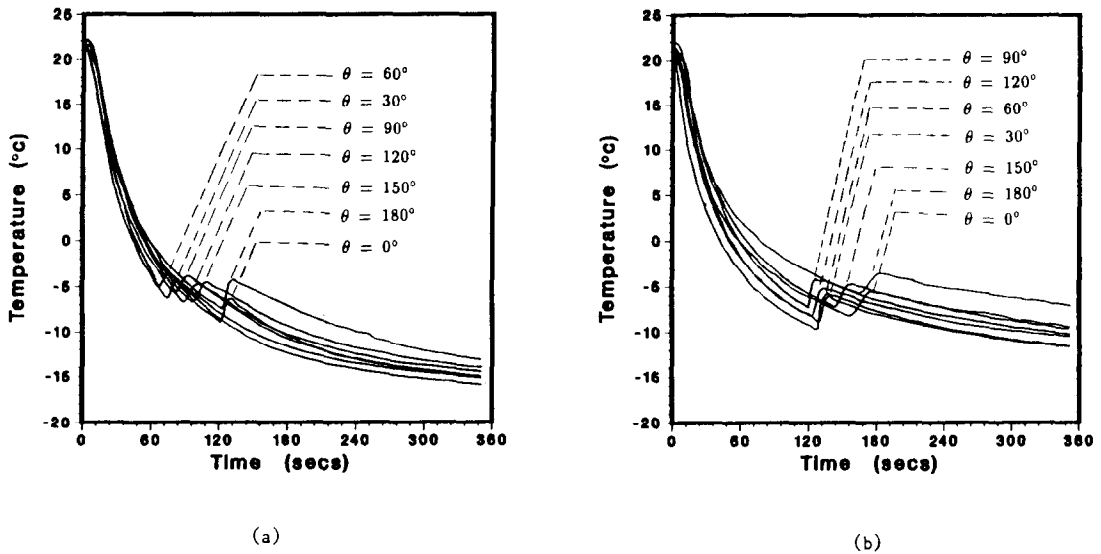


FIG. 2. The temperature variation of the cold wall: (a) glass beads; (b) steel beads.

angle is a direct result of the effect of this angle on the natural convection flow.

Next, we focus our attention on the temperature field evolving in the system as the freezing in the water-saturated porous medium takes place. Characteristic temperature profiles at the centerline perpendicular to the cold wall of the cavity are reported in Figs. 4 and 5 for the glass beads and the steel beads, respectively. The symbols represent the experimental data whereas the lines represent the predictions of a simple conduction-based theoretical model. No details of this model are given here for they can be found in the literature [14, 15]. However, for clarity, the major assumptions contained in the model are mentioned: (a) the presence of the buoyancy-driven convection is neglected; (b) the water-saturated porous medium is

considered to be semi-infinite, i.e. the presence of the surrounding walls is not taken into consideration; (c) the cold wall temperature is taken as constant throughout the freezing process and it equals the plateau value of the experimental data; (d) all the physical properties of the water-saturated porous medium are calculated as volume-weighted effective properties.

In all cases, the temperature increases as we move away from the cold wall. The solidified region at the centerline is represented by the portion of the temperature distribution below the fusion temperature (0°C). The liquid region is represented by the portion of the temperature distribution above the fusion temperature. From Figs. 4 and 5, it can be observed that the temperature profile is practically linear in the frozen region at all times for all the angles of inclination. However, the temperature profile in the unfrozen region soon becomes non-linear, signifying the presence of buoyancy-driven convection. Clearly, the natural convection is more pronounced at early times when the driving temperature difference in the system is large (Figs. 4 and 5). Furthermore, the presence of natural convection is more visible in the water-glass bead system (Fig. 4) than in the water-steel bead system (Fig. 5). The physical explanation for this finding is as follows. The effective thermal conductivity of the water-steel bead matrix is much higher than that of the water-glass bead matrix. As a result, it cannot sustain large temperature gradients which are necessary in order to drive a significant natural convection flow.

The predictions of temperature field from the theoretical model show discrepancy when compared to the experimental data, more so in the unfrozen region, especially at early times when the driving temperature differences are large and convection is important. In

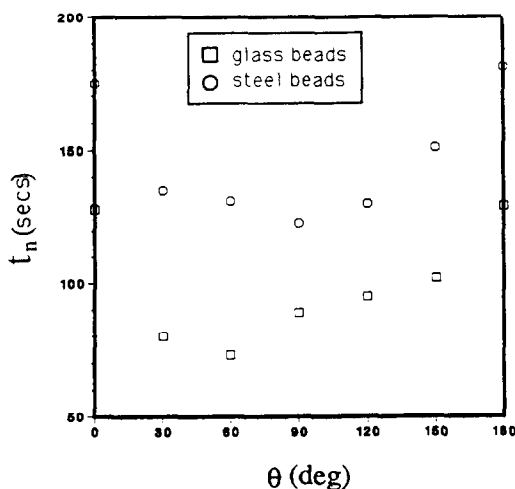


FIG. 3. The dependence of the ice nucleation time on the inclination angle.

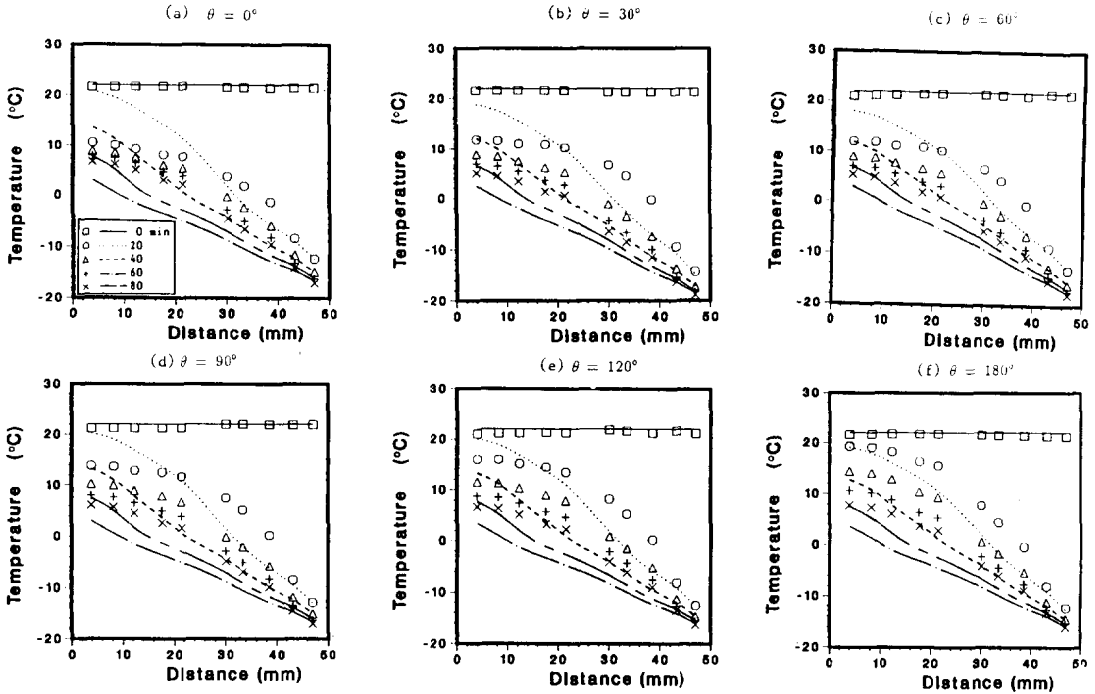


FIG. 4. Temperature distribution at the vertical centerline of the glass bead bed. The symbols denote the experimental data and the lines the theoretical prediction.

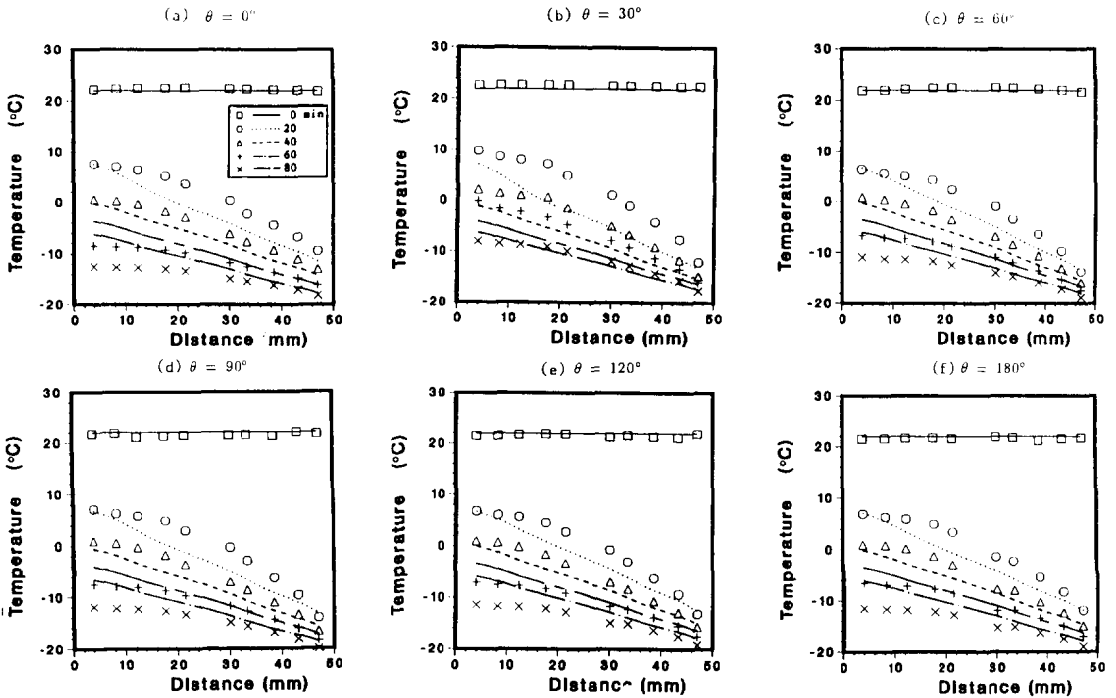


FIG. 5. Temperature distribution at the vertical centerline of the steel bead bed. The symbols denote the experimental data and the lines the theoretical prediction.

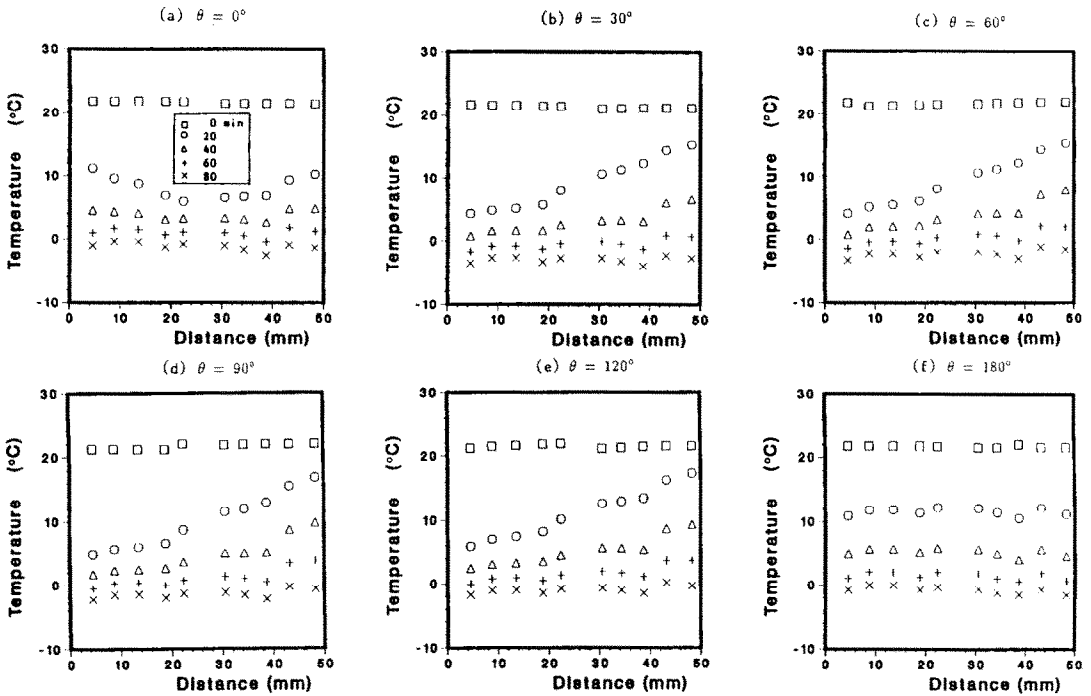


FIG. 6. Temperature distribution at the centerline of glass bead bed parallel to the cold wall.

addition, the theoretical model performs better in the case of the steel beads (Fig. 5) where conduction is dominant even in the liquid phase.

The temperature distribution at the centerline of the system parallel to the cold wall is shown in Figs. 6 and 7. Note that no results from the theoretical model are shown here since the performance of

the model was evaluated earlier and since the theoretical temperature distribution along this centerline (parallel to the cold wall) can be inferred from the temperature distribution along the centerline perpendicular to the cold wall (Figs. 4 and 5).

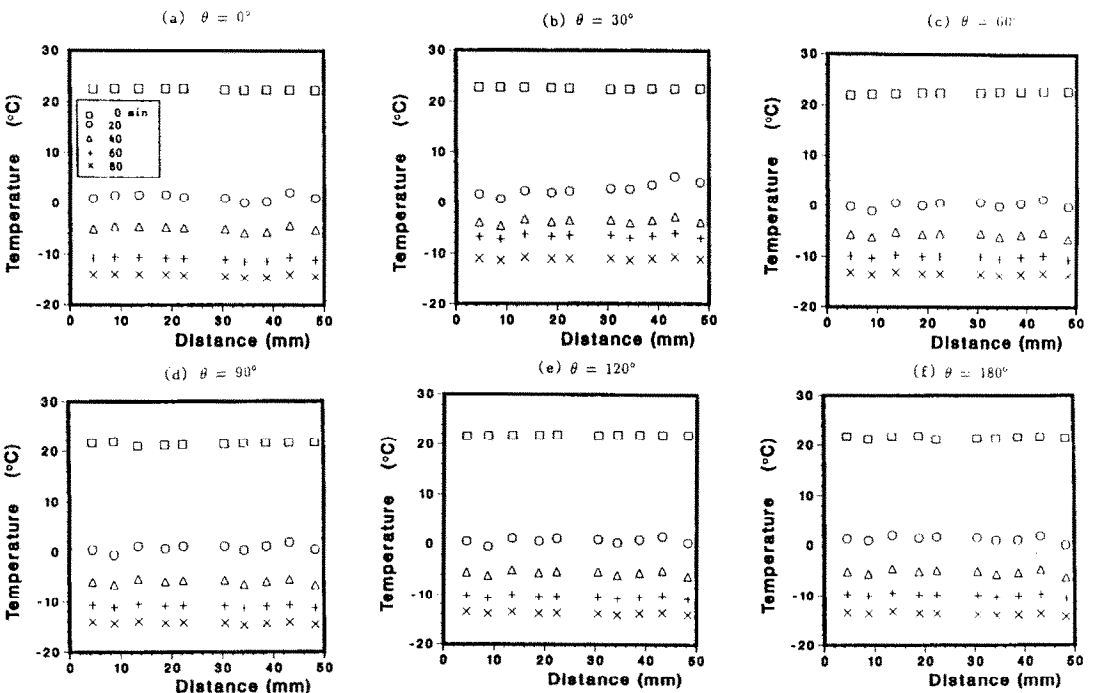


FIG. 7. Temperature distribution at the centerline of steel bead bed parallel to the cold wall.

The temperature distribution at $t = 20$ and 40 min in Fig. 6 (glass beads) as well as the flow visualization indicate the presence of bicellular flow in the system for most inclination angles of interest except $\theta = 180^\circ$. The temperature profiles for inclination angles other than $\theta = 0^\circ$ and 180° do not show any noticeable change in the convection pattern. The convection pattern in all these cases ($\theta = 30^\circ, 60^\circ, 90^\circ, 120^\circ$) is characterized by the existence of a small and weak cell to the left and a relatively larger and stronger cell to the right. For $\theta = 0^\circ$, the temperature distribution indicates the existence of two convective cells of approximately equal size located symmetrically about the centerline of the system. At $\theta = 180^\circ$, even though the cold wall is located on the underside, a flow exists, caused by the unstable stratification owing to the presence of the density extremum of water at 4°C . However, this flow is not strong enough to alter considerably the diffusion like temperature profile.

In the case of the steel bead bed (Fig. 7), the effect of convection is not prominent and the freezing phenomenon is conduction dominated. As a result, the temperature field has no appreciable dependence on the inclination angle (Figs. 7(a)–(f)). Furthermore, the temperature along the centerline parallel to the cold wall in the steel bead matrix is always lower compared to the glass bead matrix at any given time. This is a direct result of the fact heat is transported faster in the steel bead bed compared to the glass bead bed.

The main results of the growth of the phase-change

interface are shown in Figs. 8 and 9 for the glass beads and the steel beads, respectively. The interfaces in these figures were traced by using the photographs taken during the experiments. It is clear from Fig. 8 (glass beads) and Fig. 9 (steel beads) that even though the ice nucleation is delayed in the steel bead matrix (Fig. 2), the freezing progresses significantly faster in the steel bead matrix compared to the glass bead matrix. The interfaces are planar and smoother in the steel bead bed compared to the glass bead bed where they are undulated, indicating the effect of the buoyancy-driven flow at the interface shape. Owing to the high thermal conductivity of the steel matrix, the phase-change process seems to be dominated by the heat conduction in the solid beads. In the glass bead system, the freezing process is governed by heat transfer in the liquid as well as in the solid (glass beads). Note that the ratio of the thermal conductivity of water to that of glass is of the order of unity.

A result of engineering interest is the dependence of the volume of the solidified region on time and on the inclination angle. This result is shown in Fig. 10 for both the systems of interest. Note that the solidified volume fraction is normalized with respect to the total volume of the cavity ($V^* = V/V_T$).

The solidified volume increases monotonically with time for all angles in both beds of beads. After about 60 min the water saturating the steel bead matrix is completely frozen for all angles. At the same time the glass bead bed for $\theta = 0^\circ$ is only about 40% frozen. To quantify the dependence of the solidified volume

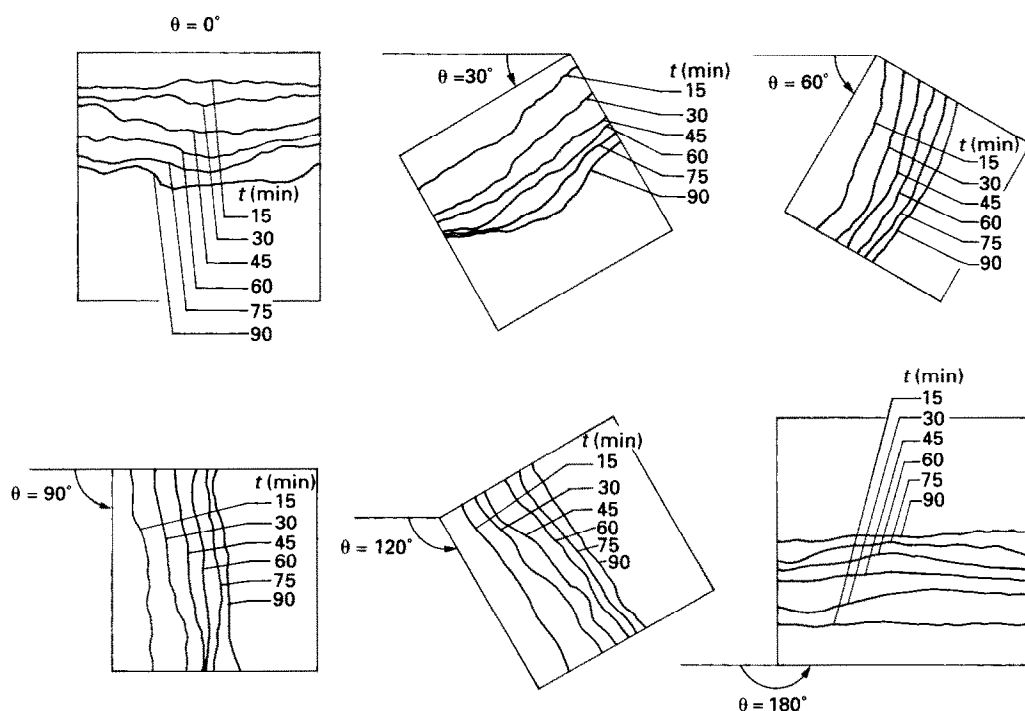


FIG. 8. The growth of the ice-water interface in the glass bead bed for different inclination angles.

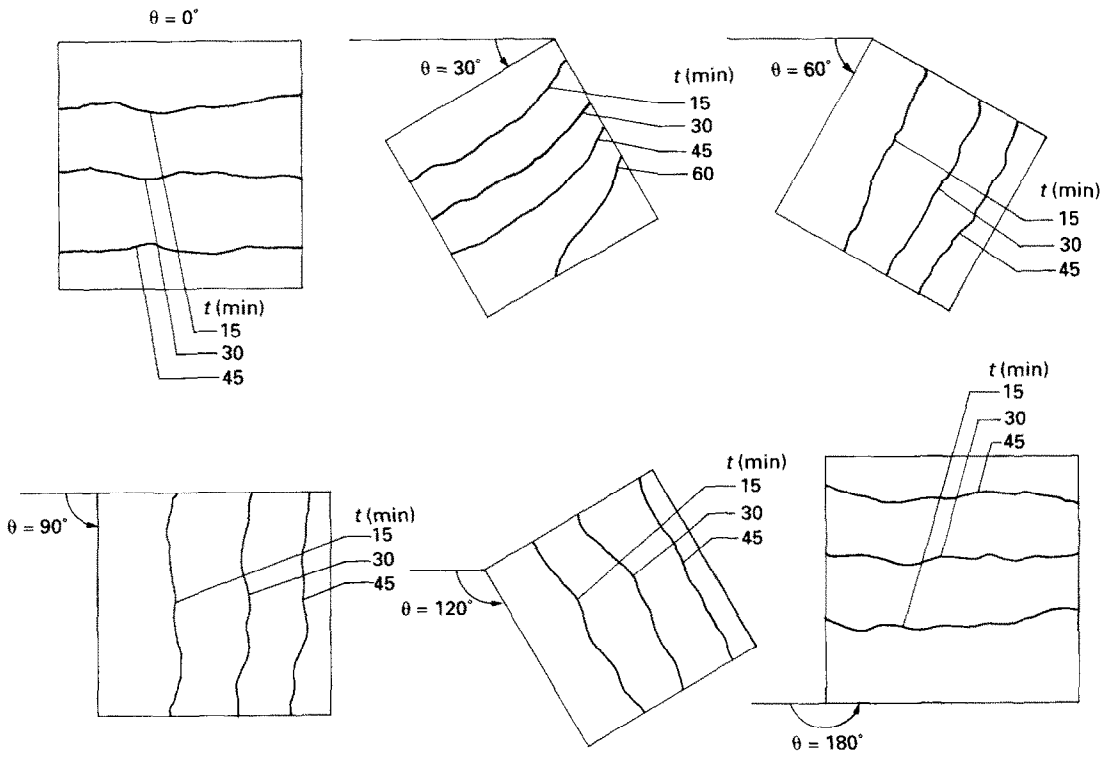


FIG. 9. The growth of the ice-water interface in the steel bead bed for different inclination angles.

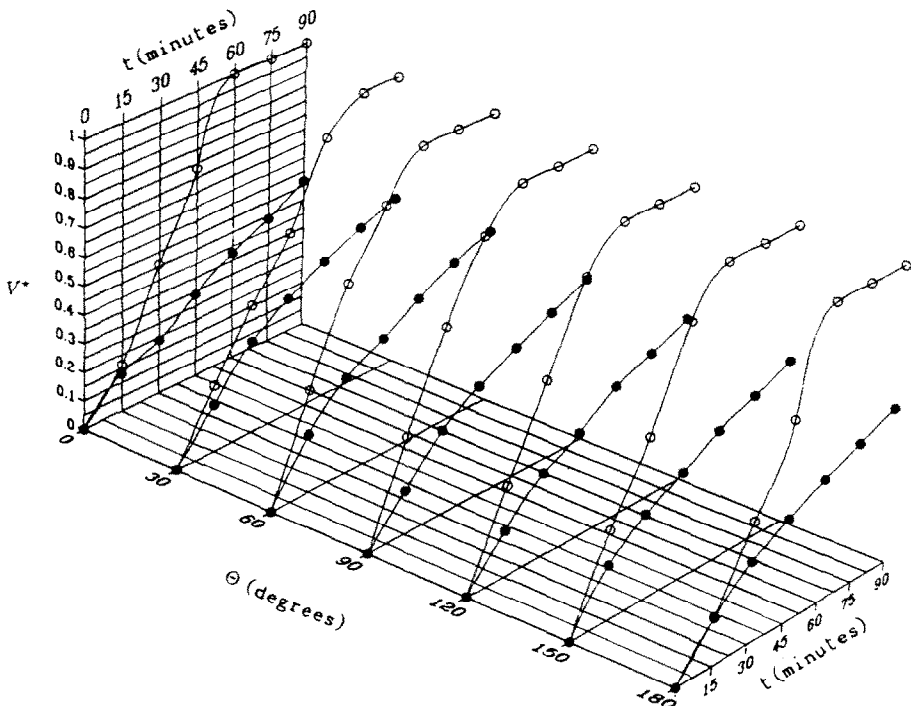


FIG. 10. The dependence of the volume of the frozen region on time and on the inclination angle. The dark circles denote the glass bead bed and the open circles the steel bead bed.

fraction on time as well as on the inclination angle, two correlations are obtained using regression analysis [16] corresponding to the data in Fig. 10 for each system. To this end, the dimensionless time was defined as

$$\tau = \frac{\alpha_{ms} t}{H^2} \frac{(T_i - T_f) C_{ms}}{L} = Fo Ste. \quad (1)$$

In the above equation, α_{ms} and C_{ms} are average quantities obtained using the parallel model [17]. Note that the dimensionless time τ is the product of the Fourier number multiplied by the Stefan number.

The following correlations were obtained for the

dependence of V^* on τ and θ :

for the glass bead system: $0^\circ < \theta < 180^\circ, 0 < \tau < 0.4$

$$V^* = 1.0752\tau^{0.6182} e^{-0.1336 \cos(\theta + 74.23)} \quad (2)$$

for the steel bead system: $0^\circ < \theta < 180^\circ, 0 < \tau < 0.5$

$$V^* = 1.5872\tau^{0.9366} e^{-0.4218 \cos(\theta + 74.23)}. \quad (3)$$

The above correlations are plotted together with the data in Figs. 11(a) and (b). It is felt that both correlations perform rather well for engineering estimates of the fraction of the solidified volume of the system.

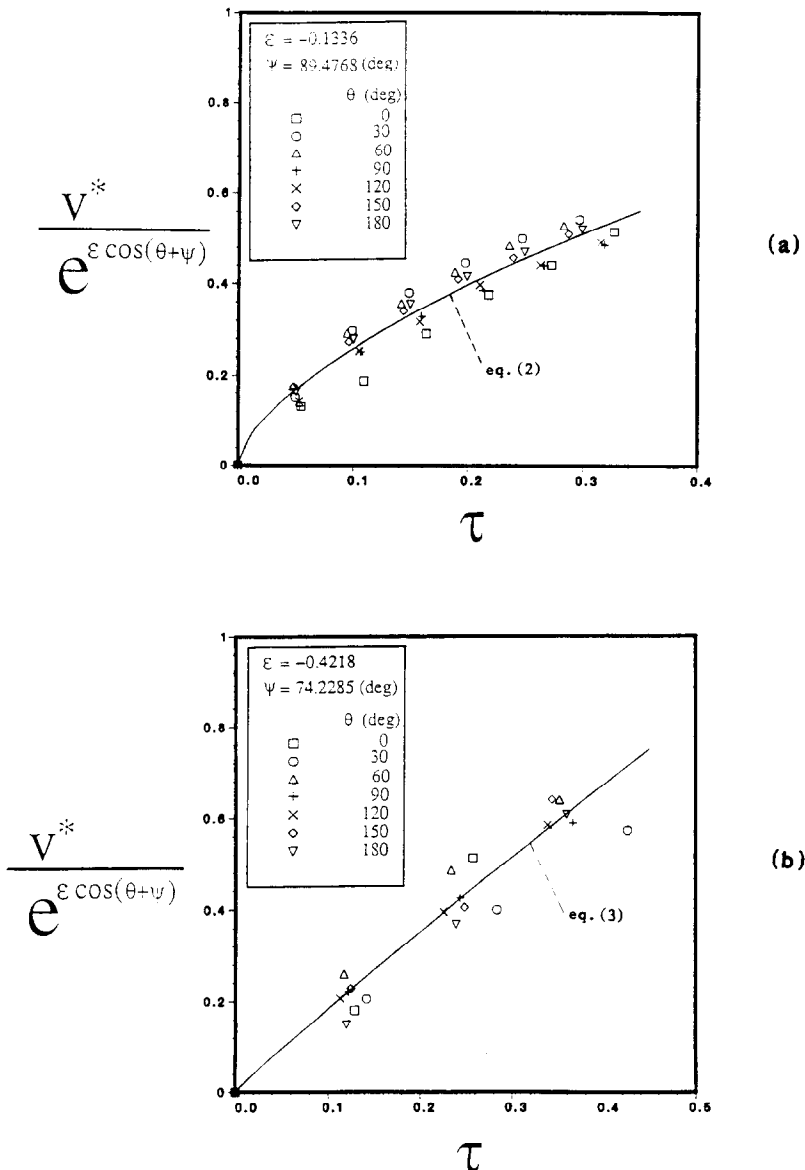


FIG. 11. A comparison between the proposed correlations (equations (2) and (3)) and the experimental data for the volume of the frozen region: (a) glass beads; (b) steel beads.

4. CONCLUSIONS

This paper presented the results of an experimental study on the transient freezing of a water-saturated inclined packed bed of beads. Two such beds were examined, one consisting of 5 mm glass beads and the other of 5 mm stainless steel beads. The results obtained show that the temperature of the cold wall exhibits a jump at the time of ice nucleation in both the systems of interest. After this jump, the cold wall temperature decreased monotonically until it leveled off. A dependence of the ice nucleation time on the angle of inclination was determined for the glass beads as well as for the steel beads. The ice nucleation was delayed in the steel bead bed compared to the glass bead bed. However, the freezing progressed much faster in the steel bead bed.

Temperature profiles along the centerline perpendicular and parallel to the cold wall testified to the presence of a buoyancy-driven flow in the system. The effect of this convective flow was more prominent in the glass bead system compared to the steel bead system where conduction was dominant at all times. A simple conduction-based theoretical model did not compare well with the experimental data in the unfrozen region in the glass bead matrix. The temperature distribution showed a dependence on the inclination angle for the glass beads whereas the temperature field did not depend markedly on the inclination angle in the steel beads where conduction was the dominating mode of heat transfer.

The growth of the phase-change interface was also observed. This interface was undulated in the glass bead system signifying the effect of the buoyancy-driven flow. To quantify the dependence of the volume of the frozen region on the inclination angle and on time, two engineering correlations were obtained (one for the glass bead system and one for the steel bead system).

Acknowledgement—Partial support for this research by the National Science Foundation (Grant No. ENG 84-51144) is gratefully acknowledged.

REFERENCES

1. M. E. Staff, Seasonal thermal energy storage, *Mech. Engrg* **105**(3), 28–34 (1983).
2. F. J. Sanger, Ground freezing in construction, *ASCE Mech. Found. Des.* **94**, 131–158 (1968).
3. V. J. Lunardini, *Heat Transfer in Cold Climates*. Van Nostrand Reinhold, New York (1981).
4. P. D. Metz, A simple computer program to model three-dimensional underground heat flow with realistic boundary conditions, *ASME J. Solar Energy Engrg* **105**, 42–49 (1983).
5. O. Svec, L. E. Goodrich and J. H. L. Planar, Heat transfer characteristics of inground heat exchanger, *J. Energy Res.* **7**, 263–278 (1983).
6. M. E. Goldstein and R. L. Reid, Effect of fluid flow on freezing and thawing of saturated porous media, *Proc. R. Soc. Lond. Series A* **364**, 45–73 (1978).
7. H. T. Hashemi and C. M. Sliepcevich, Effect of seepage stream on artificial soil freezing, *ASCE Mech. Found. Des.* **99**(1), 267–289 (1973).
8. P. E. Frivik and G. Comini, Seepage of heat flow in soil freezing, *ASME J. Heat Transfer* **104**, 323–328 (1982).
9. K. O'Neill and M. R. Albert, Computation of porous media natural convection flow and phase change. In *Finite Elements in Water Resources* (Edited by J. P. Leible, C. A. Brebbia, W. Gray and G. Pinder), pp. 213–229. Springer, Berlin (1989).
10. J. A. Weaver and R. Viskanta, Freezing of liquid-saturated porous media, *ASME J. Heat Transfer* **108**, 654–659 (1986).
11. J. A. Weaver and R. Viskanta, Freezing of water porous media in a rectangular cavity, *Int. Commun. Heat Mass Transfer* **13**, 245–252 (1986).
12. S. Chellaiah and R. Viskanta, Freezing of saturated and superheated liquid in porous media, *Int. J. Heat Mass Transfer* **31**, 321–330 (1988).
13. S. Chellaiah and R. Viskanta, Freezing of water-saturated porous media in the presence of natural convection: experiments and analysis, *ASME J. Heat Transfer* **111**, 425–432 (1989).
14. H. S. Carslaw and J. C. Jaeger, *Conduction of Heat in Solids* (2nd Edn). Oxford University Press, New York (1959).
15. M. N. Ozisik, *Heat Conduction*. Wiley, New York (1980).
16. N. R. Draper and H. Smith, *Applied Regression Analysis* (2nd Edn). Wiley, New York (1981).
17. A. Bejan, *Convection Heat Transfer*, p. 353. Wiley, New York (1984).